Acta Crystallographica Section D
Biological Crystallography
ISSN 0907-4449

Structure of an archaeal alanine:glyoxylate aminotransferase

Haruhiko Sakuraba,[a] Kazunari Yoneda,[b] Kiyo Takeuchi,[a] Hideaki Tsuge,[c] Nobuhiko Katunuma[d] and Toshihisa Ohshima[d]*

[a]Department of Life System, Institute of Technology and Science, The University of Tokushima, 2-1 Minamijosanjima-cho, Tokushima 770-8506, Japan, [b]Department of Bioscience, School of Agriculture, Kyushu Tokai University, Aso, Kumamoto 869-1404, Japan, [c]Institute for Health Sciences, Tokushima Bunri University, Tokushima 770-8514, Japan, and [d]Microbial Genetics Division, Institute of Genetic Resources, Faculty of Agriculture, Kyushu University, 6-10-1 Hakozaki, Higashi-ku, Fukuoka 812-8581, Japan

Correspondence e-mail: ohshima@agr.kyushu-u.ac.jp

Received 24 December 2007
Accepted 11 March 2008

PDB Reference: alanine:glyoxylate aminotransferase, 2zc0, r2zc0sf.

The crystal structure of a novel alanine:glyoxylate aminotransferase from the hyperthermophilic archaeon *Thermococcus litoralis* was determined at 2.3 Å resolution. The asymmetric unit contains four homologous subunits and the functional tetramer is generated by noncrystallographic 222 symmetry. Although the main-chain coordinates of the monomer of the *Thermococcus litoralis* enzyme showed a high degree of similarity to those of aspartate aminotransferase from *Thermus thermophilus* HB8, the amino-acid residues involved in substrate binding in the aspartate aminotransferase are only partially conserved in the *Thermococcus litoralis* enzyme. This may account for the difference in the substrate specificities of the two enzymes.

1. Introduction

Alanine:glyoxylate aminotransferase (AGT; EC 2.6.1.44) catalyzes the transfer of the α-amino group of L-alanine to glyoxylate, forming glycine and pyruvate. The enzyme is widely distributed among eukarya (Noguchi *et al.*, 1978; Takada & Noguchi, 1985; Sakuraba *et al.*, 1991), where one of its functions is the detoxification of glyoxylate. In humans, primary hyperoxaluria type 1 is an autosomal recessive disease caused by a deficiency in liver-specific peroxisomal AGT (Noguchi & Takada, 1979; Danpure, 2001). In bacteria, aminotransferases that catalyze transamination between L-alanine and glyoxylate have only been found in a few organisms (Koide *et al.*, 1977; Herbert & Macfarlane, 1980). These bacterial enzymes have not yet been well characterized and their physiological function remains unknown.

We recently identified a novel glyoxylate reductase in the hyperthermophilic archaeon *Thermococcus* (*Tc.*) *litoralis* (Ohshima *et al.*, 2001). This was the first biochemical evidence of an enzyme that is involved in glyoxylate metabolism in hyperthermophilic archaea. During the course of screening for enzymes associated with glyoxylate metabolism, we found a high level of AGT activity in the crude extract of *Tc. litoralis*. The presence of AGT had not yet been described for archaea, so we purified the AGT from *Tc. litoralis*, characterized it and cloned the gene that encodes it (Sakuraba *et al.*, 2004). This enzyme showed a high degree of specificity for L-alanine and glyoxylate as the amino-group donor and acceptor, respectively; however, alignment of the amino-acid sequences revealed that *Tc. litoralis* AGT bore little similarity to any other AGT described to date. When we constructed a phylogenetic tree based on the amino-acid sequence alignment of 51 species of aminotransferase reported by Mehta *et al.* (1993) and *Tc. litoralis* AGT, we found that our enzyme was clustered with aspartate, alanine, tyrosine, histidinol-phosphate and phenylalanine aminotransferases and classified into subgroup I (Sakuraba *et al.*, 2004). Eukaryal AGTs are classified into subgroup IV. We therefore proposed that the *Tc. litoralis* AGT is a novel form of the enzyme and that it might have evolved from an origin distinct from that of eukaryal AGTs (Sakuraba *et al.*, 2004).

In the present study, we solved the crystal structure of *Tc. litoralis* AGT and compared the architecture of the active site with that of aspartate aminotransferase (AspAT) from *Thermus* (*Tm.*) *thermophilus* HB8, which showed the highest structural similarity to

Table 1
Data-collection and refinement statistics.

Values in parentheses refer to the respective highest resolution data shell in each data set. R.m.s.d., root-mean-square deviation.

		SeMet		
	Native	Peak	Edge	Remote
Data collection				
Space group	$P2_12_12_1$	$P2_12_12_1$		
Unit-cell parameters (Å)	a = 77.7, b = 112.5, c = 207.3	a = 77.6, b = 112.0, c = 207.2		
Wavelength	1.0	0.9788	0.9794	0.9000
Maximum resolution (Å)	2.3	2.55	2.55	2.55
No. of unique reflections	79989	113412	113502	113412
Redundancy	7.1	3.6	3.7	3.6
Completeness (%)	98.0 (87.8)	99.8 (100)	99.8 (100)	99.8 (100)
$R_{\rm merge}$ (%)	7.3 (29.4)	6.9 (27.1)	6.7 (29.4)	6.9 (27.1)
$\langle I/\sigma(I)\rangle$	12.4 (5.2)	10.1 (4.1)	10.0 (3.9)	10.1 (4.1)
Refinement				
Resolution range (Å)	49.4–2.3			
$R/R_{\rm free}$ (%)	23.6/26.1			
No. of protein atoms	12448			
No. of water molecules	382			
R.m.s.d.				
Bond lengths (Å)	0.008			
Bond angles (°)	1.5			
Average B factors (Å^2)	48.6			
Ramachandran statistics (%)				
Most favoured	89.6			
Additionally allowed	10.1			
Generously allowed	0			
Disallowed	0.3			

Tc. litoralis AGT. We then evaluated the amino-acid residues that might be responsible for the difference in the substrate specificities of the two enzymes.

2. Materials and methods

2.1. Overexpression and purification of recombinant protein

The expression vector p18XB encoding *Tc. litoralis* AGT was prepared as described previously (Sakuraba *et al.*, 2004). *Escherichia coli* JM109 cells were transformed with p18XB, after which the transformants were cultivated at 310 K in SB medium containing ampicillin (50 µg ml^{-1}). After cultivation for 6 h at 310 K, 1 m*M* isopropyl β-D-1-thiogalactopyranoside (IPTG) was added to induce expression and cultivation was continued for an additional 3 h. The cells were then harvested by centrifugation, suspended in buffer (20 m*M* HEPES pH 7.0 containing 10 mg ml^{-1} lysozyme from egg white and 1 mg ml^{-1} DNase I from bovine pancreas), incubated for 10 min at 310 K and lysed by sonication. After centrifugation of the lysate (15 000*g* for 20 min), the supernatant was heated for 20 min at 353 K in the presence of 0.2 *M* sodium sulfate and 10% glycerol and then clarified by centrifugation. This supernatant was then dialyzed against 20 m*M* HEPES buffer pH 7.0 containing 10% glycerol and the dialyzate was loaded onto a SuperQ-TOYOPEARL 650M column (Tosoh, Tokyo, Japan) equilibrated with the same buffer. After washing the column with the same buffer, the protein was eluted with a linear gradient of 0–1 *M* NaCl in the same buffer. The active fractions were collected and dialyzed against 10 m*M* potassium phosphate buffer pH 7.0 containing 10% glycerol, after which the resultant protein solution was loaded onto a Cellulofine Hap column (Seikagaku Corporation, Tokyo) equilibrated with the same buffer. The column was then washed with the same buffer and the protein was eluted with a linear gradient of 10–250 m*M* potassium phosphate in the same buffer. The active fractions were pooled and the enzyme solution was dialyzed against 20 m*M* HEPES buffer pH 7.0 containing 10% glycerol and 0.2 *M* NaCl.

For expression of selenomethionyl AGT, *E. coli* B834 cells transformed with the p18XB vector were cultivated for 12 h at 310 K in LeMaster medium (LeMaster & Richards, 1985) containing seleno-

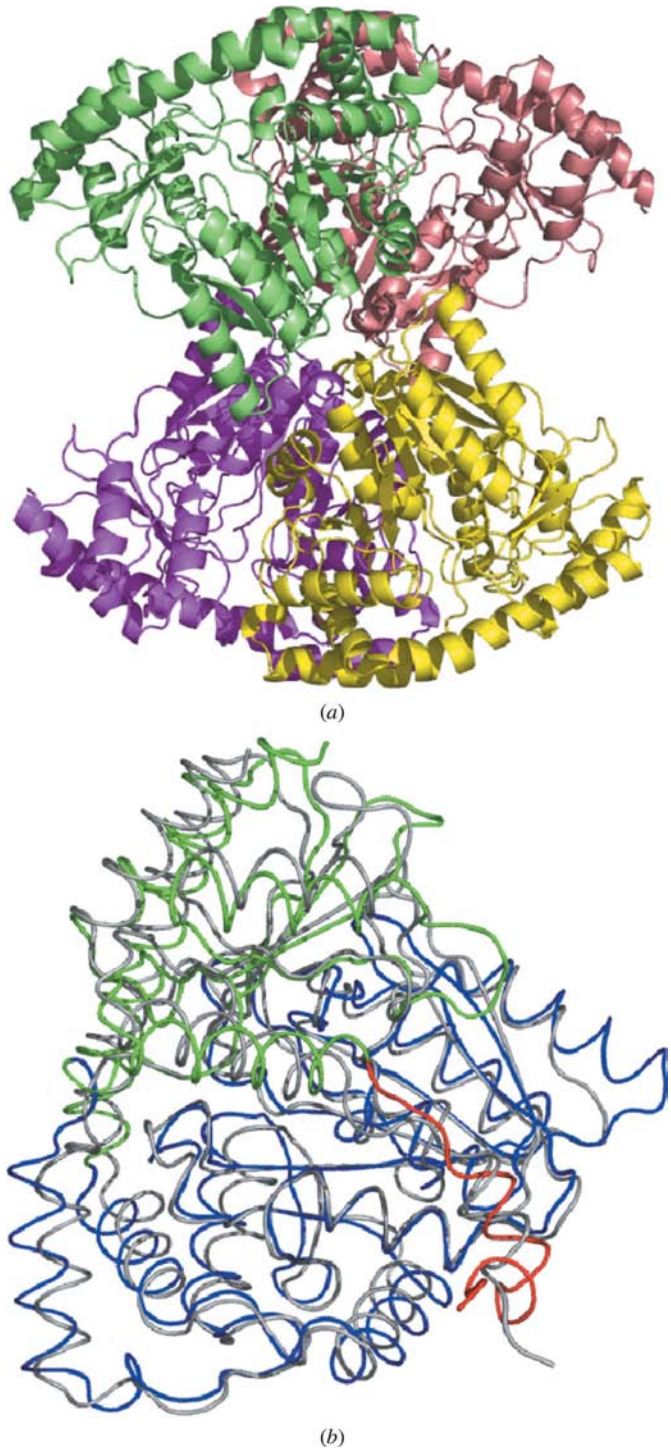

Figure 1
(*a*) Ribbon representation of the functional *Tc. litoralis* AGT tetramer, with subunits shown in different colours. (*b*) Superposition of the structures of *Tc. litoralis* AGT and *Tm. thermophilus* AspAT. For the *Tc. litoralis* AGT structure, the N-terminal arm, small domain and large domain are coloured red, green and blue, respectively. The *Tm. thermophilus* AspAT structure is shown in monochrome.

methionine. Expression was induced by the addition of 1 m*M* IPTG to the medium, after which the cultivation was continued for an additional 12 h at 310 K. The selenomethionyl AGT was purified using the same procedure as used for the native enzyme.

2.2. Crystallization and structure determination

Crystallization of the native and selenomethionyl AGT was performed using the hanging-drop vapour-diffusion method. Drops (2 µl) of protein solution (15 mg ml^{-1}) containing 5 m*M* L-alanine were mixed with an equal volume of 35–40% 1,4-butanediol, 0.1 *M* zinc acetate and 0.1 *M* imidazole–HCl pH 8.0 and equilibrated against 1.0 ml reservoir solution at 293 K. Selenium multiple-wavelength anomalous dispersion data and native diffraction data were collected on beamline BL26B1 at SPring-8. All measurements were carried out on crystals cryoprotected with 1,4-butanediol and cooled to 100 K in a stream of nitrogen gas. The data were processed using *CrystalClear* (Rigaku Corporation, Tokyo). *SOLVE* (Terwilliger & Berendzen, 1999) was used to refine the parameters of the Se atoms and to calculate the phases. The initial phases were improved by solvent flattering followed by autotracing using *RESOLVE* (Terwilliger, 1999). The model was built using *XtalView* (McRee, 1999). Refinement of the model structure was first carried out for the selenomethionyl protein diffraction data and then continued for the native diffraction data using *REFMAC*5 (Murshudov *et al*., 1997) and *CNS* (Brünger *et al.*, 1998). Pyridoxamine 5′-phosphate (PMP), imidazole, Zn^{2+} and 382 water molecules were included in the model. Because the side chains of residues 19–37 had poor electron density, these residues were represented by Ala or Gly. The two residues at the C-terminus (amino acids 406 and 407) are disordered and are not visible in the electron-density map. The model geometry was analyzed with *PROCHECK* (Laskowski *et al.*, 1993) and all the main-chain atoms except for Phe277 fell within favourable regions of the Ramachandran plot. On the basis of electron-density maps, it was confirmed that the conformation of Phe277 is correct. The *R* factor and $R_{\rm free}$ values for the final model were 23.6% and 26.1%, respectively (Table 1). Molecular-graphics figures were created using *PyMOL* (http://www.pymol.org/).

3. Results and discussion

3.1. Overall structure and structural homologues

The *Tc. litoralis* AGT protein assembled as a tetramer (Fig. 1*a*), which coincides with the subunit assembly of the enzyme in solution (Sakuraba *et al.*, 2004). The asymmetric unit consisted of four subunits related by noncrystallographic 222 symmetry. The tetramer had dimensions of about 100 × 100 × 55 Å, while the monomer had dimensions of about 55 × 55 × 45 Å. The architecture of the monomer showed the typical type 1 fold of aminotransferases, consisting of an N-terminal arm (residues 1–17), a small domain (residues 18–47 and 295–405) and a large domain (residues 48–294) (Fig. 1*b*). When we sent the model for the *Tc. litoralis* AGT monomer to the *DALI* server (Holm & Sander, 1998) to find proteins with similar structures (as of 30 October 2007), we found that the three proteins with the highest structural similarity were a putative aminotransferase from *Thermotoga maritima*, designated Tm-PAT (2.0 Å r.m.s.d. over 391 residues with 35% sequence identity; PDB code 1vp4), AspAT from *Tm. thermophilus* HB8 (2.2 Å r.m.s.d. over 374 residues with 26% sequence identity; PDB code 1bjw) and LL-diaminopimelate aminotransferase from *Arabidopsis thaliana* (2.3 Å r.m.s.d. over 353 residues with 20% sequence identity; PDB code 2z1z).

Crystal structures of AGTs from human (Zhang *et al.*, 2003), cyanobacteria (Han *et al.*, 2005), yeast (Meyer *et al.*, 2005) and mosquito (Rossi *et al.*, 2006; Han *et al.*, 2006) have been reported. When we compared the monomer structure of the *Tc. litoralis* AGT with those of other AGTs, we found that the structural similarity was extremely low (r.m.s.d. of 5.3–7.3 Å). The amino-acid sequence identity between *Tc. litoralis* AGT and the other AGTs is less than 15%. In addition, the amino-acid residues involved in cofactor binding in *Tc. litoralis* AGT (Asn186, Tyr217, Lys247 and Arg254) were not conserved in the other AGTs.

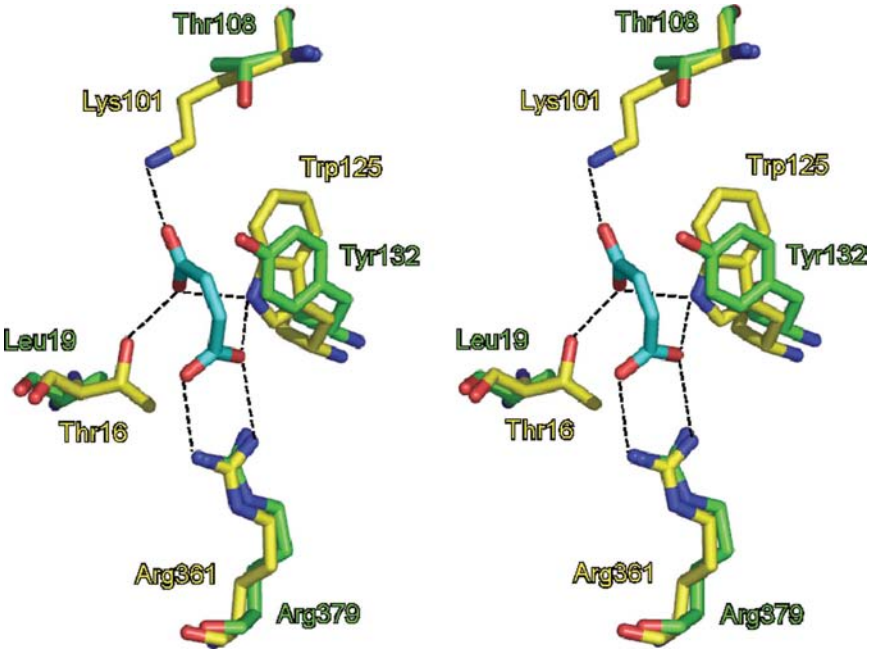

Figure 2
Stereographic close-up of the substrate-binding site. The structure of *Tc. litoralis* AGT (green) is superimposed on that of *Tm. thermophilus* AspAT (yellow). The maleate molecule is shown as a stick model in cyan. The putative interactions are shown by dotted lines. N and O atoms are shown in blue and red, respectively.

3.2. Active site

The crystal structure of *Tm. thermophilus* AspAT has also been determined in complex with maleate (Nakai *et al.*, 1999). Superposition of this structure (PDB code 1bkg) on the structure of *Tc. litoralis* AGT enabled us to compare the amino-acid residues involved in cofactor and substrate binding (Fig. 1*b*). The amino-acid residues involved in cofactor binding to *Tm. thermophilus* AspAT are Asn175, Tyr206, Lys234 and Arg242. These four residues are well conserved in *Tc. litoralis* AGT as Asn186, Tyr217, Lys247 and Arg254, respectively. In contrast, the amino-acid residues involved in substrate binding are only partially conserved (Fig. 2). The guanidino group of Arg361 in *Tm. thermophilus* AspAT forms a salt bridge with one carboxylate of the maleate, corresponding to the α-carboxylate of the substrate. This residue is conserved as Arg379 in *Tc. litoralis* AGT. Thus, the residue that

recognizes the α-carboxylate of the substrate is essentially the same in the two enzymes. On the other hand, Lys101, which forms a salt bridge with the side-chain carboxylate of the maleate in AspAT, is replaced by Thr108 in *Tc. litoralis* AGT. In addition, Thr16 and Trp125, which are directly hydrogen-bonded to the side-chain carboxylate in AspAT, are replaced by Leu19 (represented by Ala in our model) and Tyr132, respectively, in the *Tc. litoralis* enzyme.

Tm. thermophilus AspAT can react with two types of substrate that have very different properties: acidic substrates, such as aspartate and glutamate, and neutral substrates, such as alanine (Nobe *et al.*, 1998). In view of the crystal structure of the enzyme, it has been proposed that Lys101 (Lys109 in the cited reference) is the key residue involved in recognizing the side-chain carboxylate of the substrate (Nakai *et al.*, 1999). Because replacement of Lys101 with Val or Ser resulted in a loss of activity towards acidic substrates but a marked increase in activity towards alanine, it was proposed that Lys101 is a major determinant of the acidic substrate specificity of AspAT (Nobe *et al.*, 1998). We found that Lys101 is replaced by Thr108 in the structure of *Tc. litoralis* AGT. This substitution may be at least partially responsible for the marked specificity for L-alanine shown by *Tc. litoralis* AGT.

When we compared the amino-acid sequences of aminotransferase homologues for which enzymatic properties have previously been determined, we found that *Tc. litoralis* AGT exhibits highest identity (41.8%) to the human kynurenine aminotransferase-II homologue from *Pyrococcus horikoshii* OT-3 (phKAT-II). This enzyme reportedly catalyzes the transamination of kynurenine using 2-oxoglutarate as an amino-group acceptor (Chon, Matsumura, Shimizu *et al.*, 2005). In addition, comparison of the active site of *Tc. litoralis* AGT with that of the recently determined phKAT-II (PDB code 1x0m; Chon, Matsumura, Koga *et al.*, 2005) showed that Thr108 and Leu19 in *Tc. litoralis* AGT are replaced by Gln and Val, respectively, in phKAT-II, although Arg379 and Tyr132 are conserved. It would therefore be of interest to test whether phKAT-II possesses AGT activity.

In the present study, we observed a high degree of structural similarity between *Tc. litoralis* AGT and *Tm. thermophilus* AspAT, although there were key differences between the active-site residues of the two enzymes. Our results may provide critical information that will facilitate a better understanding of the substrate-recognition mechanism of subgroup I aminotransferases. At this stage, the structural features of *Tc. litoralis* AGT responsible for the strict specificity for L-alanine as an amino-group donor and glyoxylate as an amino-group acceptor remain unclear. The structure of the tertiary complex with substrate bound and mutational analyses will be the focus of further investigation.

We thank Drs M. Kanagawa, Y. Kitamura and S. Kuramitsu for help in data collection at SPring-8 beamline BL26B1. This work was supported in part by a grant from the 'National Project on Protein Structural and Functional Analysis' promoted by the Ministry of Education, Science, Sports and Culture of Japan.

References

Brünger, A. T., Adams, P. D., Clore, G. M., DeLano, W. L., Gros, P., Grosse-Kunstleve, R. W., Jiang, J.-S., Kuszewski, J., Nilges, M., Pannu, N. S., Read, R. J., Rice, L. M., Simonson, T. & Warren, G. L. (1998). *Acta Cryst.* D**54**, 905–921.
Chon, H., Matsumura, H., Koga, Y., Takano, K. & Kanaya, S. (2005). *Proteins*, **61**, 685–688.
Chon, H., Matsumura, H., Shimizu, S., Maeda, N., Koga, Y., Takano, K. & Kanaya, S. (2005). *Acta Cryst.* F**61**, 319–322.
Danpure, C. J. (2001). *The Molecular and Metabolic Bases of Inherited Disease*, edited by C. R. Scriver, A. L. Beaudet, W. S. Sly, D. Valle, B. Childs, K. W. Kinzler & B. Vogelstein, pp. 3323–3367. New York: McGraw–Hill.
Han, G. W. *et al.* (2005). *Proteins*, **58**, 971–975.
Han, Q., Robinson, H., Gao, Y. G., Vogelaar, N., Wilson, S. R., Rizzi, M. & Li, J. (2006). *J. Biol. Chem.* **281**, 37175- 37182.
Herbert, R. A. & Macfarlane, G. T. (1980). *Arch. Microbiol.* **128**, 233–238.
Holm, L. & Sander, C. (1998). *Nucleic Acids Res.* **26**, 316–319.
Koide, Y., Honma, M. & Shimomura, T. (1977). *Agric. Biol. Chem.* **41**, 781–784.
Laskowski, R. A., MacArthur, M. W., Moss, D. S. & Thornton, J. M. (1993). *J. Appl. Cryst.* **26**, 283–291.
LeMaster, D. M. & Richards, F. M. (1985). *Biochemistry*, **24**, 7263–7268.
McRee, D. E. (1999). *J. Struct. Biol.* **125**, 156–165.
Mehta, P. K., Hale, T. I. & Christen, P. (1993). *Eur. J. Biochem.* **214**, 549–561.
Meyer, P., Liger, D., Leulliot, N., Quevillon-Cheruel, S., Zhou, C. Z., Borel, F., Ferrer, J. L., Poupon, A., Janin, J. & van Tilbeurgh, H. (2005). *Biochimie*, **87**, 1041–1047.
Murshudov, G. N., Vagin, A. A. & Dodson, E. J. (1997). *Acta Cryst.* D**53**, 240–255.
Nakai, T., Okada, K., Akutsu, S., Miyahara, I., Kawaguchi, S., Kato, R., Kuramitsu, S. & Hirotsu, K. (1999). *Biochemistry*, **38**, 2413–2424.
Nobe, Y., Kawaguchi, S., Ura, H., Nakai, T., Hirotsu, K., Kato, R. & Kuramitsu, S. (1998). *J. Biol. Chem.* **273**, 29554–29564.
Noguchi, T., Okuno, E., Takada, Y., Minatogawa, Y., Okai, K. & Kido, R. (1978). *Biochem. J.* **169**, 113–122.
Noguchi, T. & Takada, Y. (1979). *Arch. Biochem. Biophys.* **196**, 645–647.
Ohshima, T., Nunoura-Kominato, N., Kudome, T. & Sakuraba, H. (2001). *Eur. J. Biochem.* **268**, 4740–4747.
Rossi, F., Garavaglia, S., Giovenzana, G. B., Arcà, B., Li, J. & Rizzi, M. (2006). *Proc. Natl Acad. Sci. USA*, **103**, 5711–5716.
Sakuraba, H., Fujiwara, S. & Noguchi, T. (1991). *Arch. Biochem. Biophys.* **286**, 453–460.
Sakuraba, H., Kawakami, R., Takahashi, H. & Ohshima, T. (2004). *J. Bacteriol.* **186**, 5513–5518.
Takada, Y. & Noguchi, T. (1985). *Biochem. J.* **231**, 157–163.
Terwilliger, T. C. (1999). *Acta Cryst.* D**55**, 1863–1871.
Terwilliger, T. C. & Berendzen, J. (1999). *Acta Cryst.* D**55**, 849–861.
Zhang, X., Roe, S. M., Hou, Y., Bartlam, M., Rao, Z., Pearl, L. H. & Danpure, C. J. (2003). *J. Mol. Biol.* **331**, 643–652.